Molecular Biology of the Cell
Vol. 14, 2071–2087, May 2003

# p38 Mitogen-Activated Protein Kinase Mediates Cell Death and p21-Activated Kinase Mediates Cell Survival during Chemotherapeutic Drug-induced Mitotic Arrest

**Karl Deacon,*† Pratibha Mistry,‡ Jonathan Chernoff,§ Jonathan L. Blank,* and Rajnikant Patel‡‖**

*Departments of Cell Physiology and Pharmacology, and ‡Biochemistry, University of Leicester, Leicester LE1 7RH, United Kingdom; and §The Fox Chase Cancer Center, Philadelphia, Pennsylvania 19111

Submitted October 14, 2002; Revised November 22, 2002; Accepted December 27, 2002
Monitoring Editor: Marc Mumby

Activation of the mitotic checkpoint by chemotherapeutic drugs such as taxol causes mammalian cells to arrest in mitosis and then undergo apoptosis. However, the biochemical basis of chemotherapeutic drug-induced cell death is unclear. Herein, we provide new evidence that both cell survival and cell death-signaling pathways are concomitantly activated during mitotic arrest by microtubule-interfering drugs. Treatment of HeLa cells with chemotherapeutic drugs activated both p38 mitogen-activated protein kinase (MAPK) and p21-activated kinase (PAK). p38 MAPK was necessary for chemotherapeutic drug-induced cell death because the p38 MAPK inhibitors SB203580 or SB202190 suppressed cell death. Dominant-active MKK6, a direct activator of p38 MAPK, also induced cell death by stimulating translocation of Bax from the cytosol to the mitochondria in a p38 MAPK-dependent manner. Dominant active PAK suppressed this MKK6-induced cell death. PAK seems to mediate cell survival by phosphorylating Bad, and inhibition of PAK in mitotically arrested cells reduced Bad phosphorylation and increased apoptosis. Our results suggest that therapeutic strategies that suppress PAK-mediated survival signals may improve the efficacy of current cancer chemotherapies by enhancing p38 MAPK-mediated cell death.

## INTRODUCTION

During mitosis, a feedback mechanism called the spindle or mitotic checkpoint ensures that replicated chromosomes are segregated equally between the two daughter cells before division (reviewed in Shah and Cleveland, 2000). The mitotic checkpoint pathway is regulated by a group of evolutionarily conserved genes that include MAD1, MAD2, MAD3 (or BUBR1), BUB1, BUB3, and MPS1 (Burke, 2000). These proteins preferentially bind to the kinetochores of unattached chromosomes where they are thought to generate the signal that suppresses anaphase onset (Burke, 2000; Shah and Cleveland, 2000). Currently, there are two ways in which the mitotic checkpoint can be activated experimentally. First, cells can be treated with chemicals that perturb microtubule dynamics such as nocodazole, taxol, vincristine, and vinblastine (Li and Benezra, 1996; Sorger *et al.*, 1997). By either depolymerizing (nocodazole, vincristine, and vinblastine) or stabilizing (taxol) microtubules, these agents activate the mitotic checkpoint and induce a mitotic cell cycle arrest (Sorger *et al.*, 1997). Second, overexpression of the MAD (mitotic arrest deficient) checkpoint proteins has been reported to activate the spindle checkpoint and cause mitotic arrest (Fang *et al.*, 1999; Geley *et al.*, 2001). Regardless of the method of activation, a common feature of the checkpoint-arrested cells is a tendency to undergo apoptotic cell death. For example, many agents used to activate the mitotic checkpoint experimentally are also used clinically in the treatment of cancer (Rowinsky and Donehower, 1991; Wilson and Jordan, 1995) and induce apoptosis in the mitotically arrested cells (Woods *et al.*, 1995; Jordan *et al.*, 1996). Therefore, the available evidence links activation of the mitotic checkpoint with apoptosis, although the biochemical mechanisms

Article published online ahead of print. Mol. Biol. Cell 10.1091/mbc.E02–10–0653. Article and publication date are at www.molbiolcell.org/cgi/doi/10.1091/mbc.E02–10–0653.

† Present address: AstraZeneca R&D Charnwood, Bakewell Road, Loughborough, Leicester, LE11 5RH, United Kingdom.
‖ Corresponding author. E-mail address: rp31@le.ac.uk.

and signaling pathways that underlie the toxicity of chemotherapeutic drugs are not clearly understood.

Studies in mammalian cells suggest that members of the mitogen-activated protein kinase (MAPK) family and the p21-activated kinase (PAK) family are involved in the regulation of cell survival and cell death (Xia *et al.*, 1995; Verheij *et al.*, 1996; Kummer *et al.*, 1997; Potapova *et al.*, 1997; Aoshiba *et al.*, 1999; Bueno *et al.*, 2000; Communal *et al.*, 2000; Kurokawa *et al.*, 2000; Remacle-Bonnet *et al.*, 2000; Schurmann *et al.*, 2000; Tang *et al.*, 2000; Deschesnes *et al.*, 2001; Gnesutta *et al.*, 2001; Jakobi *et al.*, 2001). MAPKs comprise a family of serine/threonine protein kinases that function as critical mediators of signal transduction (Kyriakis and Avruch, 2001) and include the extracellular signal-regulated kinases (ERKs), the c-Jun $NH_2$-terminal kinases (JNKs), and the p38 MAPKs. The ERKs are activated in response to mitogen or growth factor stimulation, whereas the JNKs and p38 MAPKs are activated by proinflammatory cytokines and a variety of cellular stresses, including UV light, hyperosmolarity, heat shock, and microtubule disrupting drugs (Wang *et al.*, 1998, 2000; Yujiri *et al.*, 1999; Kyriakis and Avruch, 2001; Okano and Rustgi, 2001; McDaid and Horwitz, 2001; Stadheim *et al.*, 2001). The PAKs are a group of serine/threonine protein kinases that are directly activated by the GTPases Rac and Cdc42. Together with Ras, these GTPases also activate mitogen-activated protein (MAP) kinase pathways and regulate diverse cellular processes such as cell morphology, motility, transformation, and apoptosis (Bagrodia and Cerione, 1999).

In the current study, we have examined the function of p38 MAPK in mitotically arrested HeLa cells. We show that antimicrotubule drugs cause concomitant activation of a p38 MAPK-mediated proapoptotic signaling pathway and a PAK-mediated prosurvival signaling pathway in the mitotically arrested cells. p38 MAPK stimulates apoptosis in mitotically arrested cells by inducing translocation of the proapoptotic protein Bax from the cytoplasm to the mitochondria, whereas PAK opposes p38 MAPK-induced cell death by phosphorylating the proapoptotic protein Bad.

## MATERIALS AND METHODS

### *Cell Culture and Preparation of Cell Extracts*

Human cervical carcinoma cells (HeLa) were cultured as described previously (Patel *et al.*, 1999). To obtain mitotically arrested cells, an asynchronous population of HeLa cells was treated with either nocodazole (3 $\mu$M), taxol (1 $\mu$M), vincristine (1 $\mu$M), or vinblastine (1 $\mu$M) for various times (0–30 h). Mitotic cells were collected by mechanical shake-off, washed in Dulbecco's phosphate-buffered saline (DPBS), and lysed in the appropriate buffer, depending on the protein kinase being assayed as described previously (Patel *et al.*, 1998). Radioimmunoprecipitation (RIPA) assay buffer was used to prepare cell lysates for immunoblotting with the poly ADP-ribose polymerase (PARP) antibody. Cells remaining attached to the plates after shake-off were washed three times with DPBS (containing either nocodazole [3 $\mu$M], taxol [1 $\mu$M], vincristine [1 $\mu$M], or vinblastine [1 $\mu$M]) and lysed by scraping into the appropriate buffer. Cell lysates were centrifuged at 14,000 $\times$ *g* for 10 min at 4°C, and the protein content of the supernatant was determined using the Coomassie protein assay reagent (Pierce Chemical, Rockford, IL) before normalization and solubilization in two times SDS-PAGE sample buffer. Cell lysates for Western blotting with the Bad antibody or the phospho-specific Bad antibodies were solubilized in SDS-PAGE sample buffer before sonication for 10–15 s.

### *Antibodies*

p38$\alpha$, Erk1, Erk2, cdk1, anti-hemagglutinin epitope tag (HA), and PAK$\alpha$ were purchased from Santa Cruz Biotechnology (Santa Cruz, CA). Anti-FLAG (M2), Cy3-conjugated anti-FLAG (M2), anti-$\gamma$-tubulin, anti-$\beta$-actin, horseradish peroxidase (HRP)-conjugated goat anti-mouse, HRP-conjugated goat anti-rabbit, and HRP-conjugated mouse anti-goat were from Sigma-Aldrich (St. Louis, MO). Anti-JNK1 (BD Biosciences PharMingen, San Diego, CA) anti-M30, which detects caspase cleavage, and cytokeratin 18 (Leers *et al.*, 1999) was from Roche Diagnostics (Indianapolis, IN), along with anti-PARP (Roche Diagnostics). Alexa Fluor 488 goat anti-mouse IgG, Alexa Fluor 488 goat anti-rabbit IgG, and Alexa Fluor 594 rabbit anti-mouse IgG were from Molecular Probes (Eugene, OR). Phosphospecific anti-Bad and total anti-Bad were from New England Biolabs (Beverly, MA).

### *Plasmids and Mutagenesis*

The expression vectors (FLAG epitope-tagged in pCDNA3) for p38$\alpha$ (murine), p38$\beta$ (human), p38$\gamma$ (human), and p38$\delta$ (human) were provided by J. Han (Scripps Research Institute, La Jolla, CA). The following expression vectors (all FLAG epitope-tagged in pCDNA3) were provided by R. Davis (University of Massachusetts Medical Center, Amherst, MA): dominant active (DA) MKK6 (S207D, T211D), kinase dead (KD) MKK6, glutathione *S*-transferase (GST)-p38$\alpha$ wild-type (WT), and GST-MKK6 (WT). The following expression constructs (all HA-epitope-tagged in the pXJ vector) were provided by E. Manser (Glaxo-Singapore, Singapore): PAK$\alpha$ (WT), DAPAK$\alpha$ (L106F), and KDPAK$\alpha$ (K298A). The expression vector for green fluorescent protein (GFP)-human bax was provided by R. Youle (National Institutes of Health, Bethesda, MD). The constructs for generating recombinant GST-fusion proteins of murine wild-type Bad (mBad) were provided by G. Bokoch (Scripps Research Institute). The mammalian expression vector for GST-mBad (pEBG-mBad) was purchased from New England Biolabs. The pEBG empty vector was provided by D. Alessi (University of Dundee, Dundee, United Kingdom). In vitro mutagenesis of mBAD was carried out using the QuickChange site-directed mutagenesis kit (Stratagene, La Jolla, CA) according to the manufacturer's protocol. Human MAD2 was cloned from a HeLa cell cDNA library (Stratagene) by polymerase chain reaction and subcloned into a mammalian expression vector (pCMV5) containing an N-terminal HA tag.

### *Immunoprecipitation and Western Blot Analysis*

Immunoprecipitations were performed as described previously (Patel *et al.*, 1998). The immunoprecipitated proteins and the cell extracts were resolved by SDS-PAGE and electroblotted onto Hybond-C nitrocellulose membrane by using a Hoeffer semidry blotting apparatus (Amersham Biosciences, Piscataway, NJ). Immunoreactive proteins were visualized using enhanced chemiluminescence (Amersham Biosciences). For immunoblotting with the phosphospecific Bad antibodies, the procedure recommended by the manufacturer was strictly followed.

### *Protein Kinase Assays*

Immunecomplex kinase assays for JNK1, p38 MAPK, Erk1, Erk2, and cdk1 were performed as described previously (Patel *et al.*, 1998) using GST-c-Jun, GST-activating transcription factor-2 (ATF-2), myelin basic protein (MBP), and histone H1 as substrates, respectively. The activity of the immunoprecipiated PAK$\alpha$ was assayed as described above for JNK1 (Patel *et al.*, 1998) by using a GST-fusion containing the N-terminal 290 amino acids of mitogen-activated protein kinase kinase kinase (MEKK)2 as substrate (Deacon and Blank, 1999; Hagemann and Blank, 2001). Incorporated radioactivity was quantified by liquid scintillation counting of bands excised from SDS-PAGE gels.

### Flow Cytometry

Analysis of the DNA content was performed by flow cytometry (FACScan; BD Biosciences, San Jose, CA) as described previously (Patel *et al.*, 1998).

### Transfection of HeLa Cells

HeLa cells were plated at a density of $\sim 5 \times 10^5$ cells/well in a six-well plate or at $1 \times 10^5$ cells/well for coverslips in an eight-well plate. Eighteen to 24 h later, the cells were transfected with 1–4 $\mu$g of DNA by using FuGENE 6 according to the manufacturer's instructions (Roche Diagnostics). At 18–24 h after transfection, the cells on the coverslips were either fixed in cold (−20°C) methanol or incubated with MitoTracker red CMXRos (500 nM; Molecular Probes) for 15 min at 37°C, washed two times with DPBS, and fixed for 10 min in 4% (vol/vol) formaldehyde in DPBS. The cells were then processed for immunofluorescence microscopy as described below. The cells in the six-well plates were either washed two times with DPBS and lysed in the appropriate buffer to make cell extracts or collected (floating and attached cells) either for flow cytometry or for the determination of apoptosis as described above.

### Immunofluorescence and Confocal Microscopy

HeLa cells were grown either on coverslips or in eight-well chambered slides (Nalge Nunc, Naperville, IL) and where indicated the cells were transfected as described above. The cells were washed three times in DPBS and fixed either in cold (−20°C) methanol for 30 min at −20°C or in 4% (vol/vol) formaldehyde in DPBS for 30 min at room temperature (for MitoTracker). Cells were rinsed five times with phosphate-buffered saline and the aldehyde-fixed cells permeabilized in 0.1% (vol/vol) Triton X-100 in phosphate-buffered saline for 10 min at room temperature. Cells were then blocked with 1% (wt/vol) bovine serum albumin (BSA) (in DPBS) for 45–60 min at room temperature. The following primary antibodies, diluted in 1% (wt/vol) BSA in DPBS, were used for immunocytochemistry: $\alpha$-FLAG (M2), $\alpha$-FLAG (M2) Cy3-conjugate, or $\alpha$-HA. After incubation at room temperature for 60 min, the cells were washed five times with DPBS before incubation with the secondary antibody for a further 60 min at room temperature. The following secondary antibodies, diluted in 1% (wt/vol) BSA in DPBS, were used: sheep anti-mouse IgG, Texas Red conjugated sheep anti-mouse IgG, fluorescein isothiocyanate-conjugated and donkey anti-rabbit IgG, fluorescein isothiocyanate-conjugated. The cells were washed five times with DPBS and the nuclei labeled by staining with Hoechst 33258 (1 $\mu$g/ml in DPBS) for 5 min at room temperature. Cells were viewed on an inverted fluorescence microscope (TE3000; Nikon, Tokyo, Japan), and images were captured through a 100× objective (numerical aperture 1.4) by using an Orca ER charge-coupled device camera (Hamamatsu Photonics, Bridgewater, NJ). For deconvolution the images were captured in the z-plane at 1-$\mu$m intervals by using a 100× piezo-driven objective (numerical aperture 1.4). The images were volume deconvolved and merged using Openlab software (Improvision, Coventry, United Kingdom). The Openlab images were subsequently compiled in Photoshop (Adobe Systems, Mountain View, CA). Confocal scanning microscopy was performed on a Leitz DM IRB/E TCS4D (Leica, Wezlar, Germany). A krypton/argon laser was used for fluorescence excitation of GFP (488 nm), MitoTracker red (568 nm), Hoechst 33342 (364 nm), and Cy5 (647 nm). Images were processed and maximum projections made using Scanware (Leica). Tiff files for all four fluorochromes were merged using OpenLab software.

### Preparation of Recombinant GST Fusion Proteins

Recombinant GST-c-Jun, GST-ATF-2, GST-MEKK2 (N terminus), GST-MKK6 (wt), and GST-p38$\alpha$ were prepared as described previously (Deacon and Blank, 1999).

### Reagents

SB203580 and SB202190 (Calbiochem, San Diego, CA). Nocodazole, taxol, vincristine, vinblastine, cytochalasin D, phorbol 12-myristate 13-acetate (PMA), anisomycin, and histone H1 (type IIIs; Sigma-Aldrich). MBP (Invitrogen, Carlsbad, CA). All other reagents were of analytical grade and obtained from Sigma-Aldrich.

## RESULTS

### p38 MAPK Is Activated Preferentially in Mitotically Blocked HeLa Cells

Treatment of HeLa cells with nocodazole (3 $\mu$M) resulted in MAD2 localization to condensed chromatin in the mitotically arrested cells, confirming that the checkpoint was activated (Figure 1A). Analysis of the nocodazole-treated cells by flow cytometry (Figure 1B) indicated the presence of two populations: a mitotic population with high cdk1 activity (Figure 2, A and B) and an attached, nonmitotic population with low cdk1 activity (Figure 2, B and C).

We evaluated the activity of the MAPKs in the nocodazole-treated cells by using immunocomplex kinase assays. p38 MAPK was activated primarily in the mitotically arrested population (Figure 2A). Immunoblot analysis of p38$\alpha$ immunoprecipitates indicated that the activation of p38 MAPK was not due to variations in the level of immunoprecipitated p38 protein. In contrast to p38 MAPK, both JNK and Erk MAP kinases were activated primarily in the attached cells (Figure 2, A and B). The activation of MAP kinase family members was evaluated further using alternative drugs that perturb microtubule dynamics and cause mitotic arrest. As observed with nocodazole, treatment of HeLa cells with either taxol (1 $\mu$M), vincristine (1 $\mu$M), or vinblastine (1 $\mu$M) caused mitotic arrest (as shown by high cdk1 activity; Figure 2C) and activated p38 MAPK selectively in the mitotically arrested population. With the exception of taxol, which activated JNK equally in both the mitotic and the attached cells, vincristine, vinblastine, and nocodazole activated JNK preferentially in the attached cells (Figure 2C). All four drugs also activated the Erk MAP kinases preferentially in the attached cell population (Figure 2C). Importantly, treatment of HeLa cells with cytochalasin D (5 $\mu$M) or EDTA (0.5 mM) to induce cell rounding or detachment did not activate p38 but did stimulate JNK activity (our unpublished data). Furthermore, p38 MAPK was selectively activated in mitotic mouse NIH3T3 cells arrested with either nocodazole, taxol, vincristine, and vinblastine (our unpublished data). These results indicate that p38 MAPK is specifically activated in mammalian cells mitotically arrested by microtubule-interfering drugs.

We also evaluated whether p38 MAPK was activated in a synchronized population of mitotic HeLa cells. In normal mitotic cells (Mit), containing high cdk1 activity, p38 MAPK activity was not detected compared with cells arrested in mitosis with nocodazole (Noc; Figure 2D). To further confirm that p38 MAPK activation was not necessary for normal mitosis, we used the p38 MAPK inhibitors SB203580 and SB202190 (Lee *et al.*, 1994). Addition of either SB203580 (20 $\mu$M) or SB202190 (10 $\mu$M) to HeLa cells 3 h after release from an aphidicolin-thymidine double block had no effect on either entry into or exit from mitosis compared with vehicle-treated control cells (our unpublished data). These results

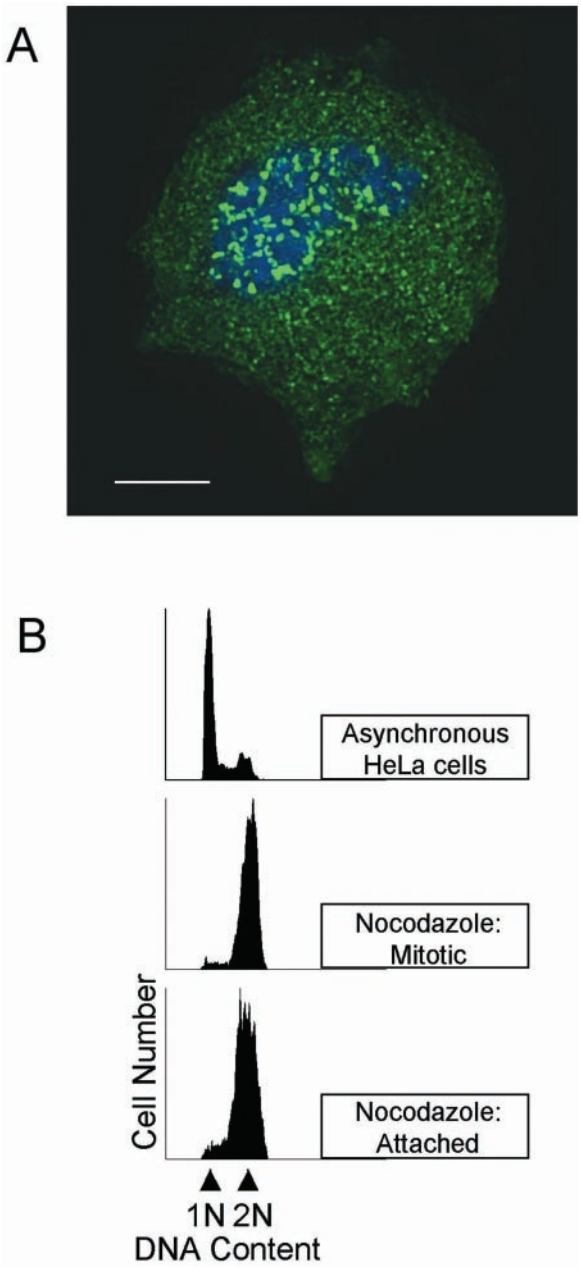


**Figure 1.** Nocodazole activates the mitotic checkpoint and causes mitotic cell cycle arrest. (A) HeLa cells were transfected with HA-MAD2 as described in MATERIALS AND METHODS. After 24 h, the cell were treated with nocodazole (3 $\mu$M) for 12 h and the mitotic cells collected by "shake-off." The mitotic cells were attached to poly-D-lysine–coated coverslips and the cells processed for immunofluorescence microscopy as described in MATERIALS AND METHODS. HA-MAD2 (green) localized to the condensed chromosomes (blue) in the nocodazole-arrested mitotic cells. Bar, 10 $\mu$m. (B) Flow cytometry DNA profiles of exponentially growing HeLa cells (top), nocodazole-arrested mitotic cells (middle), and nocodazole-treated attached cells (bottom).

suggest that p38 MAPK is unlikely to be activated during normal mitosis.

Because p38 MAPK is activated only in the mitotically arrested cells, we performed a time-course analysis of p38 activation at intervals after the addition of nocodazole (3 $\mu$M) to asynchronous HeLa cells. JNK activity was also assayed in parallel. At 6 h after nocodazole addition, when the majority of the cells was still attached (>90%), p38 MAPK activity was low, whereas JNK activity was maximal (Figure 3, A and B). From 12 h onward, we were able to collect purely mitotic cells by shake-off as assessed by high cdk1 activity. The activation of p38 MAPK correlated closely with that of cdk1, whereas JNK activity had returned to near basal levels 12 h after nocodazole addition (Figure 3, A and B). Furthermore, removal of nocodazole from the mitotically arrested cells resulted in exit from mitosis, as shown by the inactivation of cdk1. This inactivation of cdk1 correlated with the inactivation of p38 (Figure 3, C and D), providing further evidence that p38 MAPK activation is specifically associated with mitotic arrest.

### *PAK Is Also Activated Preferentially in Mitotically Arrested Cells*

We examined the activation of the PAK$\alpha$ in mitotically arrested HeLa cells. PAK$\alpha$ and p38 MAPK activity was analyzed at intervals after the addition of nocodazole (3 $\mu$M) to exponentially growing cells. PAK$\alpha$ activation paralleled p38 MAPK activation, both occurring selectively in the mitotic population at 12 h and remaining elevated for up to 30 h. Neither PAK$\alpha$ nor p38 MAPK activation was observed in the attached population over the same time period (Figure 4A). Similar results were obtained after treatment of HeLa cells with taxol (our unpublished data). HeLa cells treated with taxol (1 $\mu$M), vincristine (1 $\mu$M), or vinblastine (1 $\mu$M) also selectively activated both p38 MAPK and PAK in the mitotically arrested cells (Figure 4B). Treatment of HeLa cells with either cytochalasin D (5 $\mu$M) or EDTA (0.5 mM) did not activate PAK (our unpublished data). Furthermore, removal of the mitotic block in nocodazole-arrested cells resulted in inactivation of PAK as cells exited mitosis, as assessed by inactivation of cdk1 (Figure 4C). However, PAK inactivation seemed to be delayed relative to that of p38 MAPK. Collectively, these results suggest that activation of both PAK and p38 MAPK is specifically associated with mitotic arrest.

To determine whether PAK is an upstream activator of p38 MAPK in HeLa cells we cotransfected either wild-type (WT) or dominant active (DA) PAK (L106F) with WT p38$\alpha$. DAPAK, in comparison with WT PAK, was highly active as assessed by its ability to phosphorylate GST-Mekk2 but was unable to activate cotransfected p38$\alpha$, as measured GST-ATF2 phosphorylation (Figure 4D). The transfected p38$\alpha$ was, however, activated by anisomycin as assessed by phosphorylation of GST-ATF2. These data suggest that DAPAK is not coupled to p38 MAPK activation in HeLa cells.

### *p38 MAPK Activation Stimulates Apoptotic Cell Death, whereas PAK Activation Promotes Cell Survival*

The effect of nocodazole on cell death was assessed in both the attached and the mitotically arrested populations by

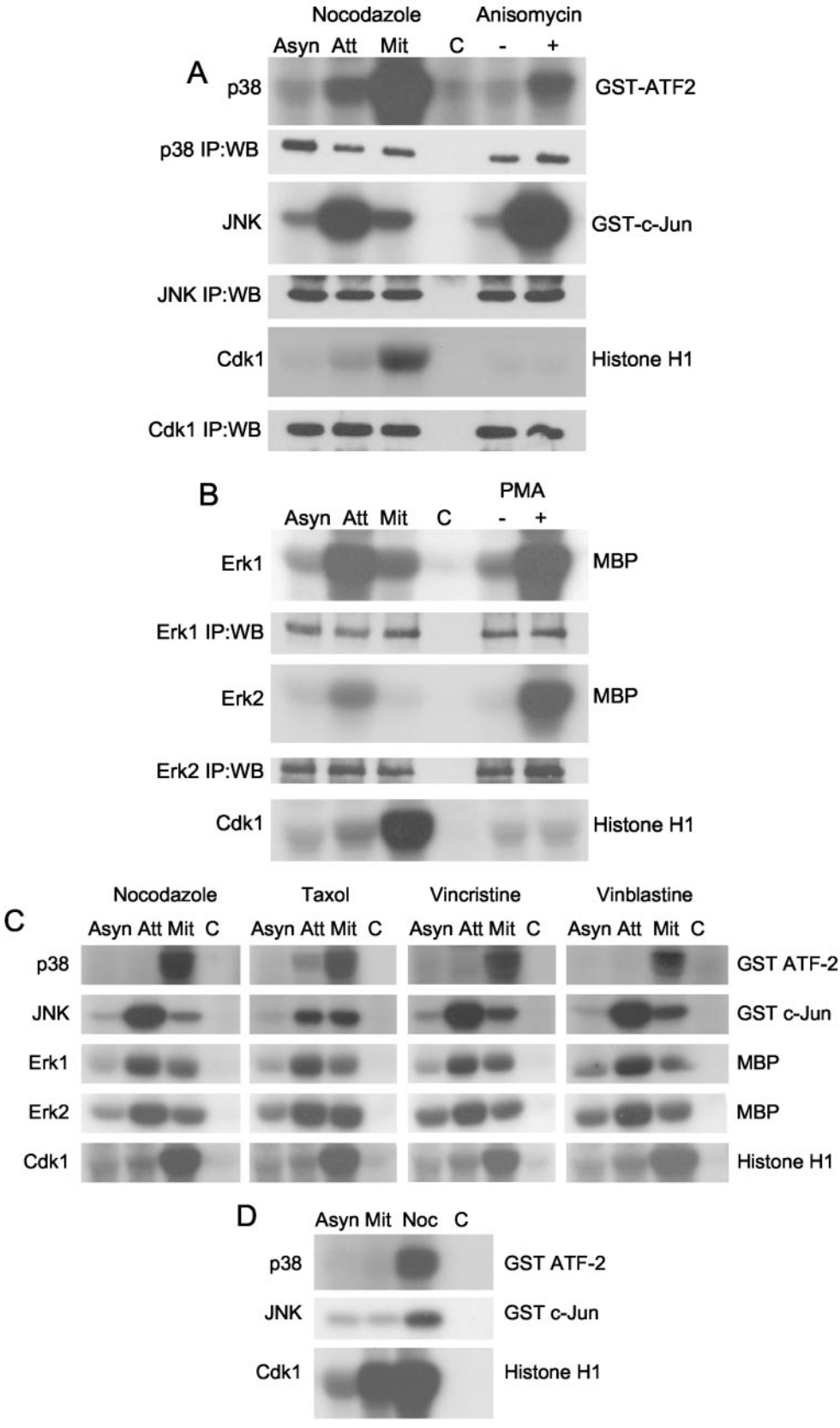


**Figure 2.** Activation of p38 MAPK, but not JNK or Erk, occurs during mitotic arrest but not during normal mitosis. (A) Exponentially growing HeLa cells were treated with either dimethyl sulfoxide alone (asynchronous population [Asyn]) or with nocodazole (3 $\mu$M) for 12 h, and the cells separated into a mitotic (Mit) and an attached (Att) population. Specific antibodies were used to immunoprecipitate (IP) p38 MAPK, JNK, and cdk1 from the cell lysates for immunocomplex kinase assays and Western blotting (WB) with anti-p38 MAPK, anti-JNK, and anti-cdk1. A sample of the mitotic cell lysate was also incubated with protein A-Sepharose beads alone (C). Protein extracts prepared from HeLa cells treated with anisomycin (100 ng/ml for 0.5 h) were also analyzed in parallel as a positive control for the activation of both p38 MAPK and JNK. (B) Activation of Erk1, Erk2, and cdk1 in nocodazole-arrested mitotic cells was determined as described above. Protein extracts from phorbol 12-myristate 13-acetate–treated (100 nM for 0.5 h) HeLa cells were also analyzed in parallel as a positive control for the activation of both Erk1 and Erk2. (C) Activation of p38 MAPK, JNK, Erk1, Erk2, and cdk1 after treatment of exponentially growing HeLa cells with either nocodazole (3 $\mu$M), taxol, vincristine, or vinblastine (all 1 $\mu$M) for 12 h. (D) HeLa cells were synchronized using the aphidicolin-thymidine double block method as described in MATERIALS AND METHODS. Eight to 10 h after release from the cell cycle block, mitotic cells were collected by shake-off and the activation of p38 MAPK, JNK, and cdk1 in this mitotic cell population (Mit) determined as described in A. Protein extracts from nocodazole-treated (3 $\mu$M for 12 h) HeLa cells were also analyzed in parallel as a positive control for the activation of p38 MAPK.

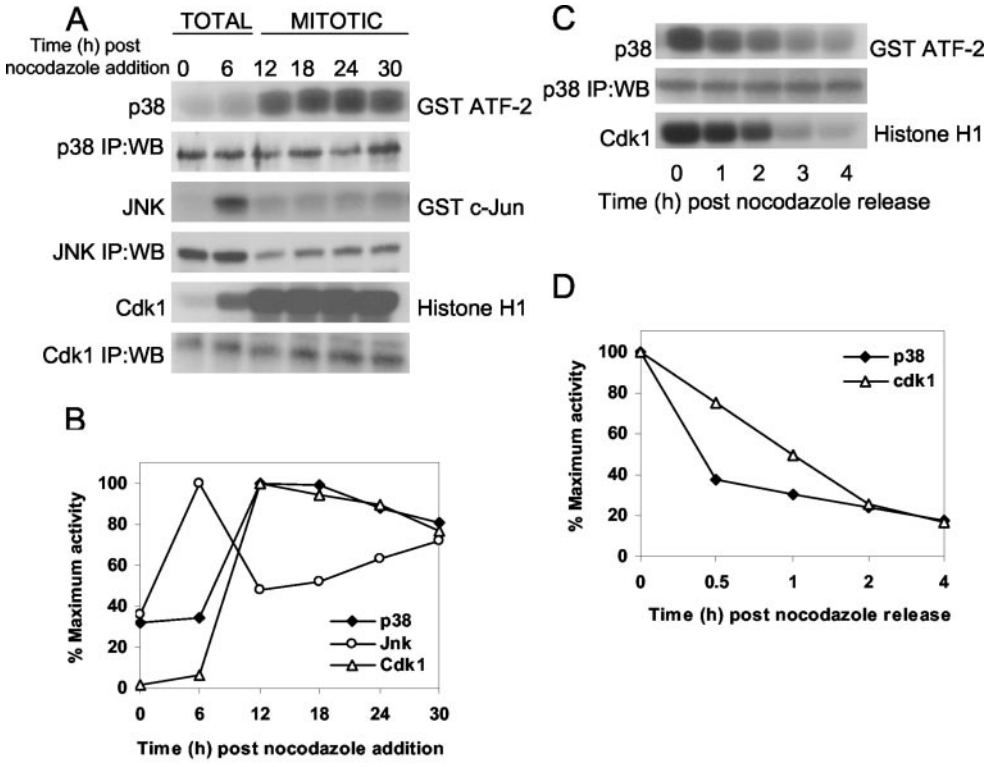


**Figure 3.** p38 MAPK activation and inactivation correlates with cdk1 activation and inactivation respectively. (A) Exponentially growing HeLa cells were treated with nocodazole (3 $\mu$M) and cell extracts prepared at the indicated time points after nocodazole addition. The activation of p38 MAPK, JNK, and cdk1 was assessed using immunocomplex kinase assays as described in MATERIALS AND METHODS. (B) Quantitation of the data shown in A. (C) Exponentially growing HeLa cells were treated with nocodazole (3 $\mu$M) for 12 h and the mitotic cells collected by shake-off. After the removal of nocodazole cell extracts were prepared at the indicated time points to assess the activation of both p38 MAPK and cdk1 using immunocomplex kinase assays as described in MATERIALS AND METHODS. (D) Quantitation of the data shown in C.

either immunoblotting with an anti-PARP antibody or immunostaining with the M30 antibody. Nocodazole-induced poly (ADP-ribose) polymerase (PARP) cleavage was apparent in the mitotic cells at 12 h after drug addition and continued to increase over the time course examined (Figure 5A). Treatment of HeLa cells with either taxol (1 $\mu$M), vincristine (1 $\mu$M), or vinblastine (1 $\mu$M) also caused PARP cleavage, preferentially in the mitotic population (Figure 5B). Nocodazole also induced cleavage of cytokeratin 18 and caused a time-dependent increase in the number of apoptotic cells specifically in the mitotic cell population (Figure 5C, right).

To determine whether p38 MAPK was involved in this apoptotic response, p38 MAPK inhibitors were used. SB203580 (20 $\mu$M) or SB202190 (10 $\mu$M) reduced the number of apoptotic cells in the mitotic population by 46 and 42%, respectively, as assessed by cytokeratin 18 cleavage (Figure 5D). The relationship between p38 MAPK activity and apoptosis was examined further by transfecting HeLa cells with dominant active (DA) MAP kinase kinase, MKK6 (S207D, T211D). Consistent with previous reports (Derijard *et al.*, 1995; Jiang *et al.*, 1997) DAMKK6 activated all coexpressed p38 MAPK isoforms (Figure 6A). Transient expression of daMKK6 in HeLa cells caused apoptosis, as assessed by cytokeratin 18 cleavage and chromatin fragmentation (Figure 6B). The DAMKK6-induced apoptosis is likely to be mediated through activation of endogenous p38 MAPK, because treatment of the transfected cells with either SB303580 (20 $\mu$M) or SB202190 (20 $\mu$M) inhibited apoptosis by ~67% (Figure 6C).

To address the function of PAK in mitotically arrested cells, DAPAK$\alpha$ (L106F) was transfected into HeLa cells, either separately or together with DAMKK6 (Figure 6D), and their effect on survival assayed using the M30 antibody. In the absence of any treatment, 2% of the cells were found to be apoptotic (Figure 6E). Transfection with the empty vector alone increased the number of apoptotic cells to 12%. In contrast, 54% of DAMKK6-transfected cells were found to be apoptotic as assessed by the presence of both cleaved cytokeratin 18 and fragmented chromatin, whereas a signaling inactive mutant of MKK6 (S207A, T211A) did not induce apoptosis (14%). Coexpression of DAPAK with DAMKK6 suppressed DAMKK6-induced apoptosis to near basal levels (18%), whereas KDPAK did not affect the level of MKK6-induced apoptosis. We also determined whether PAK aids cell survival of nocodazole-arrested mitotic cells. Treatment of DAPAK-transfected HeLa cells with nocodazole (3 $\mu$M for 24 h) reduced the number of apoptotic cells in the mitotic population by 56% (nocodazole: percentage of M30 positive cells $\pm$ SEM; 34.2 $\pm$ 3.4, n = 3; nocodazole + DAPAK: 15 $\pm$ 2.2, n = 3). These results suggest that nocodazole activates two signaling pathways in mitotically arrested cells that have opposing effects on cell survival. Activation of p38 MAPK either by nocodazole or MKK6 stimulates cell death, whereas activation of PAK stimulates cell survival.

### *DAMKK6 Induces Bax Translocation from the Cytoplasm to the Mitochondria and PAK Phosphorylates Bad*

To examine the mechanism by which p38 MAPK and PAK exert their effect on cell survival, we examined whether these enzymes regulate the activity of the bcl-2 family members Bad and Bax. The effect of p38 MAPK on the intracel-

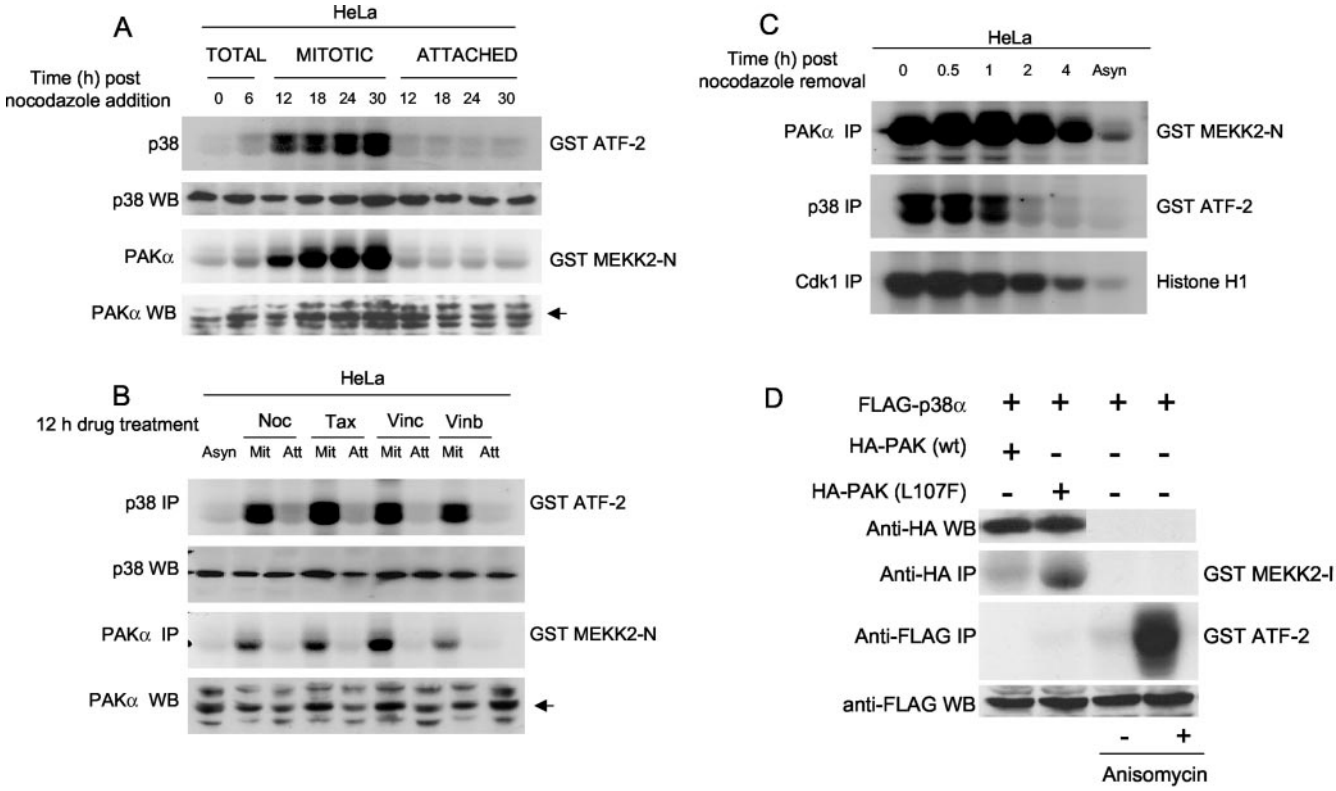


**Figure 4.** PAK activation correlates with the activation of p38 MAPK in mitotically arrested HeLa cells but PAK does not activate p38 MAPK. (A) Exponentially growing HeLa cells were treated with nocodazole (3 $\mu$M) and cell extracts prepared, after separation of the attached (Att) and the mitotic cell populations (Mit), at the indicated time points. Activation of p38 MAPK and PAK was assessed using immunocomplex kinase assays as described in MATERIALS AND METHODS. The cell extracts were also immunoblotted (WB) with specific antibodies for p38$\alpha$ and PAK$\alpha$. (B) Activation of p38 MAPK and PAK after treatment of exponentially growing HeLa cells were treated with nocodazole (3 $\mu$M), taxol, vincristine, or vinblastine (all 1 $\mu$M) for 12 h. The cell extracts were also immunoblotted (WB) with anti-p38$\alpha$ and PAK$\alpha$. (C) Activation of p38 MAPK and PAK$\alpha$ at the indicated times after treatment of exponentially growing HeLa cells were treated with nocodazole (3 $\mu$M) for 12 h. (D) HeLa cells were transfected with FLAG epitope-tagged p38$\alpha$ alone or together with either HA epitope-tagged wild-type (wt) PAK$\alpha$ or dominant active (L107F) HA-PAK$\alpha$. Twenty-four hours after transfection, cells transfected with p38$\alpha$ alone were treated with anisomycin (100 ng/ml for 0.5h) or an equivalent volume of dimethyl sulfoxide. The activation of PAK$\alpha$ and p38 MAPK was determined using immunocomplex kinase assays and cell extracts immunoblotted with either an anti-HA or anti-FLAG antibody to verify transfection efficiency.

lular distribution of Bax was investigated by cotransfecting HeLa cells with DAMKK6 and a GFP-Bax fusion construct. Both GFP-Bax (Figure 7A) and MKK6 (Figure 7B) were distributed homogeneously throughout the cytoplasm of exponentially growing cells when expressed alone. Cotransfection of GFP-Bax with DAMKK6 resulted in a dramatic change in the distribution of Bax from a homogeneous distribution to a more punctate, perinuclear distribution (Figure 7C). Early morphological changes (16 h after transfection) included cell rounding and membrane blebbing (Figure 7C). At later times (36 h after transfection), chromatin condensation and fragmentation was accompanied by cell shrinkage (Figure 7D). In control experiments where KDMKK6 was cotransfected with GFP-Bax, Bax remained homogeneously distributed throughout the cytoplasm (Figure 7E). In addition, cotransfection of DAMKK6 with a plasmid expressing GFP alone caused no redistribution of GFP (Figure 7F). To determine whether the DAMKK6-induced redistribution of Bax was mediated through activation of p38 MAPK, cells cotransfected with GFP-Bax and DAMKK6 were treated with either SB203580 or SB202190. In cells transfected with GFP-Bax alone, Bax showed a punctate, perinuclear distribution in 14% of the cells. However, in cells coexpressing both GFP-Bax and DAMKK6, 55% of the cells displayed a punctate, perinuclear distribution of Bax. In the presence of either SB203580 (20 $\mu$M) or SB202190 (10 $\mu$M) the translocation of Bax to the perinuclear region was reduced to near basal levels (16%) (Figure 7G).

We determined whether DAMKK6 was inducing redistribution of GFP-Bax to the mitochondria. In cells cotransfected with GFP-Bax and DAMKK6 (Figure 8, A–E), the punctate distribution of GFP-Bax (Figure 8A) coincided with mitochondrial staining by MitoTracker red (Figure 8B). These results demonstrate that the DAMKK6-induced activation of p38 MAPK is sufficient to stimulate Bax translocation from the cytosol to the mitochondria. Next, we determined whether Bax also translocates to the mitochondria in nocodazole-arrested mitotic cells. HeLa cells transfected with

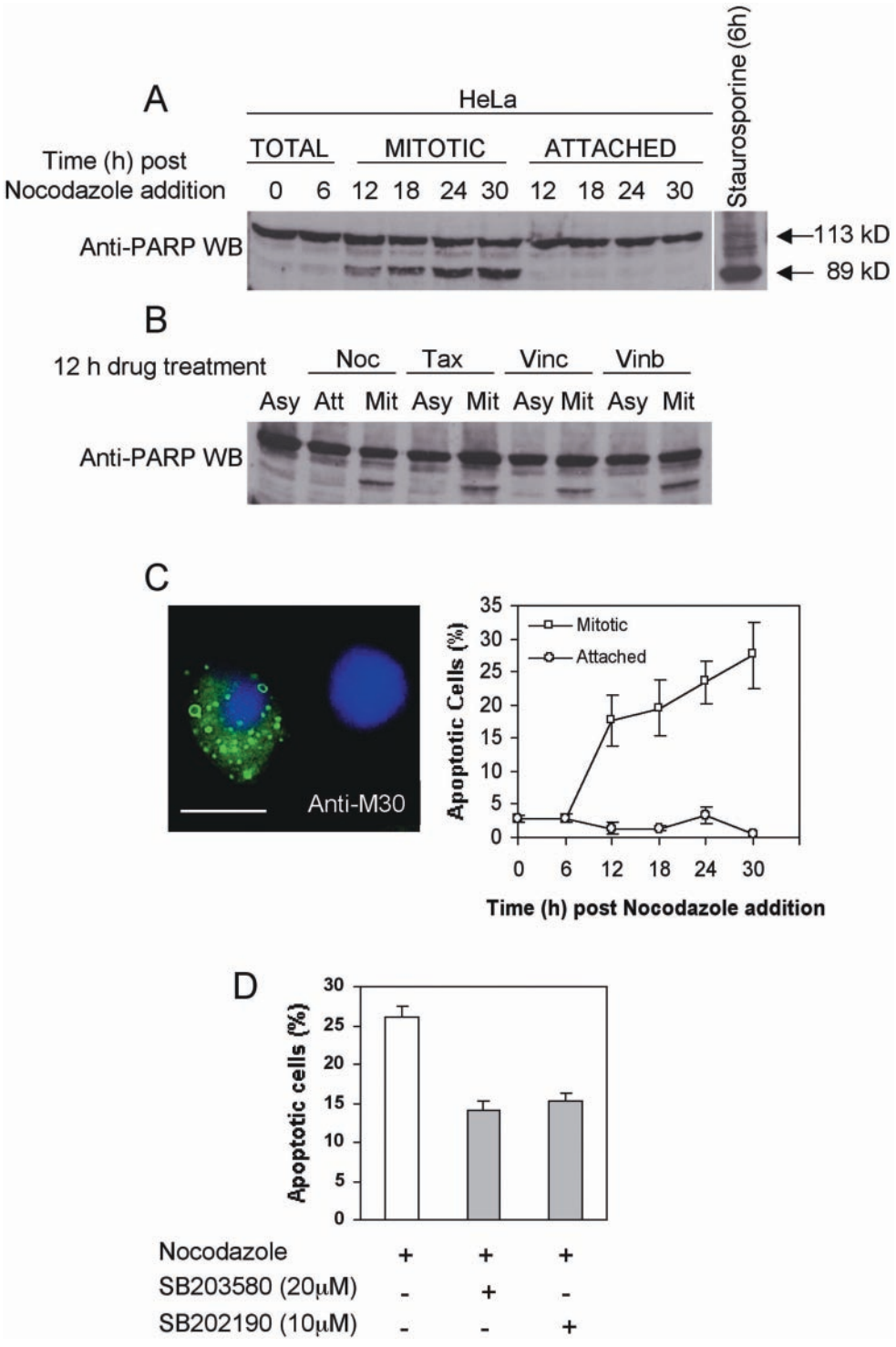


**Figure 5.** Nocodazole-mediated induction of apoptosis in HeLa cells requires p38 MAPK activity. (A) Immunoblot analysis (WB) of nocodazole-induced apoptosis, assessed by PARP cleavage, after treatment of exponentially growing HeLa cells with nocodazole (3 $\mu$M) for the indicated times. At the 6-h time point a mitotic shake-off was not performed as few mitotic cells were present (<10%). Protein extracts prepared from HeLa cells treated with staurosporine (1 $\mu$M for 6 h) were analyzed in parallel as a positive control for PARP cleavage. Arrowheads indicate the position of the immunoreactive bands corresponding to intact PARP (113 kDa) and the caspase-cleaved PARP (89 kDa). (B) Immunoblot analysis of PARP cleavage after treatment of exponentially growing HeLa cells with nocodazole (3 $\mu$M), taxol, vincristine, or vinblastine (all 1 $\mu$M) for 12 h. (C) HeLa cells were plated onto sterile glass coverslips. Twenty-four hours later, the cells were treated with nocodazole (3 $\mu$M) for the indicated times. The mitotic cells were recovered by shake-off, and the cells were reattached to poly-D-lysine–coated glass coverslips. Both the mitotic and attached cells were fixed and stained with the M30 antibody as described IN MATERIALS AND METHODS. Left, indirect immunofluorescence staining of nocodazole-arrested mitotic cells (24h treatment) with the M30 antibody (green) and the DNA stain Hoechst 33342 (blue). The cell on the right does not show M30 immunoreactivity and is not apoptotic. Bar, 10 $\mu$m. Right, quantitation of the number of M30 immunoreactive cells in the mitotic and attached cell populations, at the indicated time points, after treatment with nocodazole. At least 100 cells were counted in randomly selected fields for each time point, and the data shown represents the mean ± SEM of three independent experiments. (D) Effect of SB203580 (20 $\mu$M) and SB202190 (10 $\mu$M) on nocodazole (3 $\mu$M for 24 h)-induced apoptosis. Control cells were treated with an equivalent vol-ume of dimethyl sulfoxide. After 24 h, the mitotic cells were collected by shake-off and reattached to poly-L-lysine–coated coverslips. The cells were fixed and immunostained with the M30 antibody as described in MATERIALS AND METHODS. At least 100 cells were counted in randomly selected fields for each condition and the bars represent the mean ± SEM of three independent experiments.

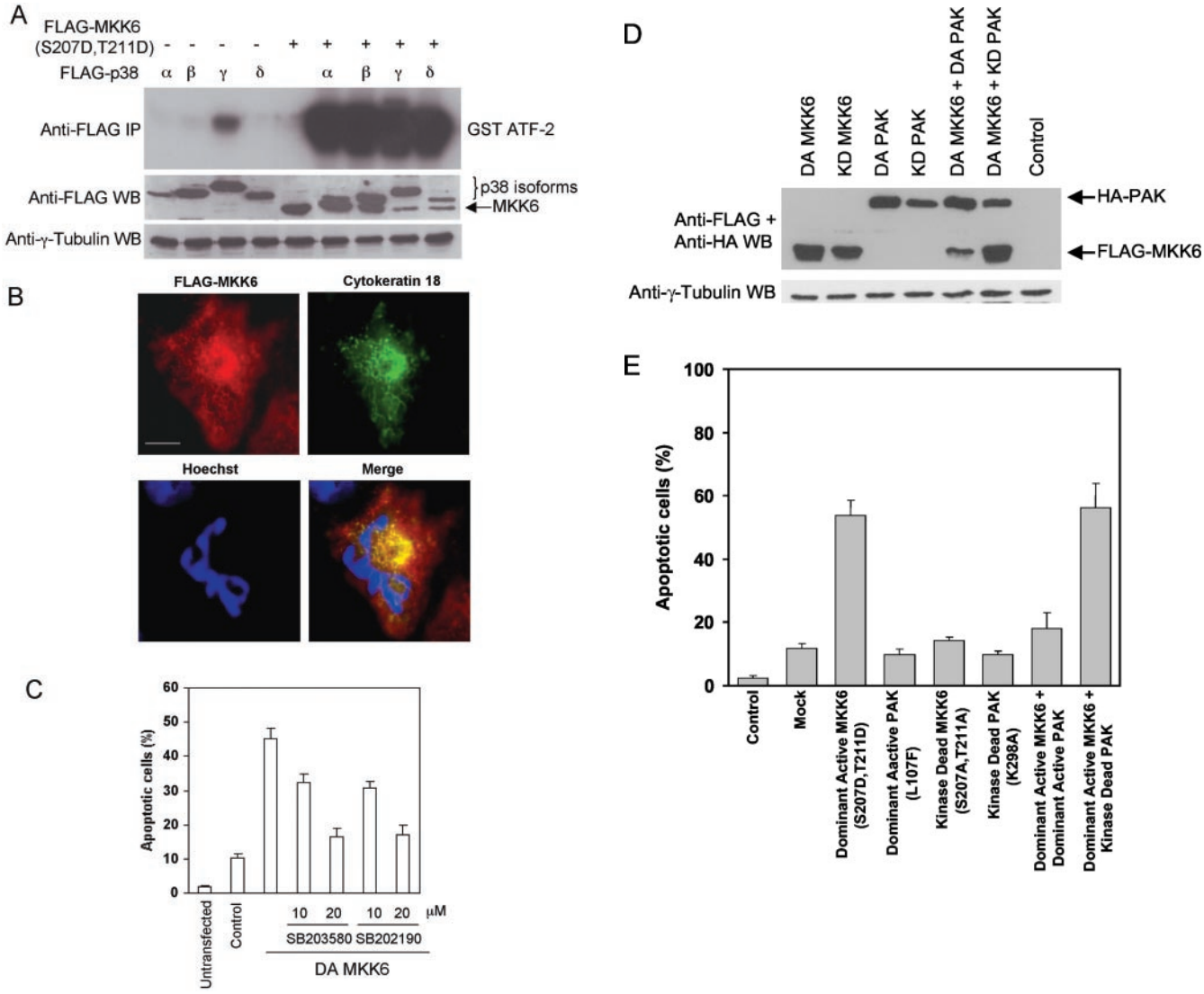


**Figure 6.** DAMKK6 induces apoptosis in HeLa cells by activating p38 MAPK, whereas DAPAK inhibits daMKK6-induced apoptosis. (A) HeLa cells were transfected with either the FLAG epitope-tagged p38 isotypes or FLAG-DAMKK6 (S207D, T211D) alone or in combination with each other. Twenty-four hours after transfection, the activation of p38 MAPK isotypes was determined using an immunocomplex kinase assay as described in MATERIALS AND METHODS. The cell extracts were also immunoblotted with either an anti-FLAG antibody or an anti-γ-tubulin antibody. The arrowhead indicates the position of FLAG-MKK6. (B) Exponentially growing HeLa cells were transfected with FLAG-DAMKK6. Twenty-four hours after transfection, the cells were fixed and immunostained sequentially with the M30 antibody and an anti-FLAG antibody as described in MATERIALS AND METHODS. Indirect immunofluorescence of an MKK6 transfected cell (top left) showing cleaved cytokeratin 18 (top right) and DNA fragmentation (bottom left). The merged image is also shown (bottom right). Bar, 10 μm. (C) HeLa cells were transfected with either FLAG-DAMKK6, empty vector alone (control) or left untransfected. Eight hours after transfection the cells were treated with either SB203580 (10–20 μM), SB202190 (10–20 μM), or with an equivalent volume of dimethyl sulfoxide alone. Twenty-four hours after transfection, the cells were fixed and immunostained with the M30 antibody as described in MATERIALS AND METHODS. At least 100 transfected cells were counted in randomly selected fields for each condition, and the bars represent the mean ± SEM of three independent experiments. (D) Exponentially growing HeLa cells were transfected with either FLAG-DAMKK6, FLAG-kinase dead (KD)MKK6, HA-DAPAK, HA-KDPAK, empty vector alone (control), or cotransfected with FLAG-DAMKK6 and HA-DAPAK or FLAG-DAMKK6 and HA-KDPAK. Twenty-four hours after transfection cell extracts were prepared and immunoblotted with either with a mixture of anti-FLAG and anti-HA antibodies or with an anti-γ-tubulin antibody. (E) Exponentially growing HeLa cells were transfected with the indicated constructs. Twenty-four hours after transfection, the cells were fixed and immunostained with an anti-FLAG antibody to identify the transfected cells and with the M30 antibody to identify the apoptotic cells as described in MATERIALS AND METHODS. At least 100 MKK6-transfected cells were counted in randomly selected fields for each condition and the bars represent the mean ± SEM of three independent experiments.

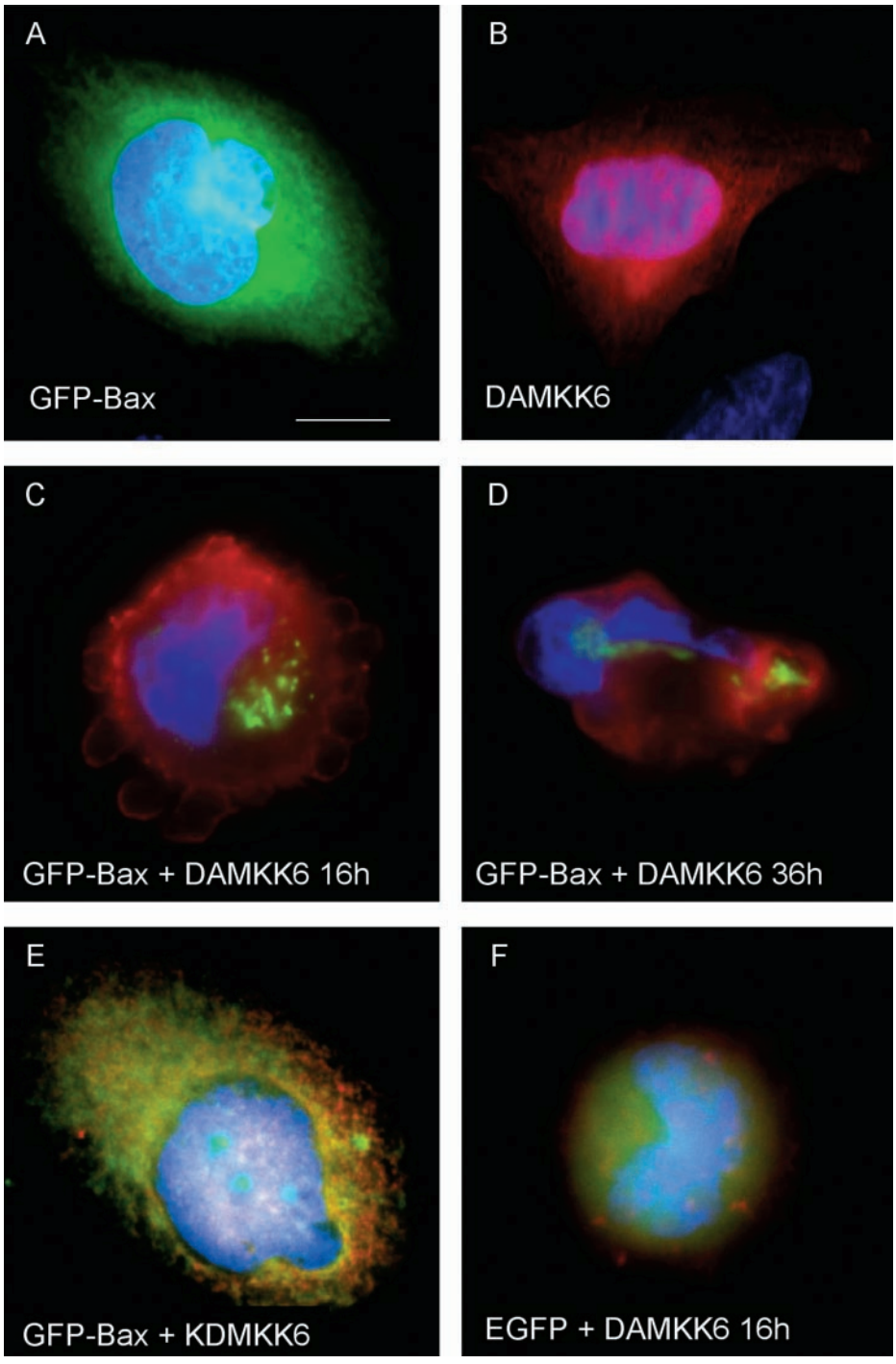


**Figure 7.** DAMKK6 induces p38 MAPK-dependent redistribution of the proapoptotic protein Bax in HeLa cells. HeLa cells were transfected with either GFP-Bax or FLAG-DAMKK6 alone or cotransfected with either GFP-Bax and FLAG-DAMKK6, GFP-Bax, and FLAG-KDMKK6 or EGFP and FLAG-DAMKK6. Sixteen hours (A–C, E, and F) or 36 h after transfection (D), the cells were fixed and immunostained with an anti-FLAG antibody to detect the MKK6 (red) and the DNA was stained with Hoechst 33342 (blue) as described in MATERIALS AND METHODS. Indirect immunofluorescence showing the intracellular distribution at 16 h after transfection of GFP-Bax (A), FLAG-DAMKK6 (B), GFP-Bax in a cell overexpressing DAMKK6 (C), GFP-bax distribution in a cell overexpressing DAMKK6 at 36 h after transfection (D), GFP-Bax intracellular localization in the presence of KDMKK6 (E), and the intracellular distribution of GFP in the presence of DAMKK6 (F). Bar, 10 $\mu$m A–C, E and F); 5 $\mu$m (D). (G) Exponentially growing HeLa cells were transfected with either GFP-Bax alone or cotransfected with GFP-Bax and FLAG-DAMKK6. Six hours after transfection the cells cotransfected with GFP-Bax and FLAG-DAMKK6 were treated with either SB203580 (20 $\mu$M) or SB202190 (10 $\mu$M). Twenty-four hours after transfection, the cells were fixed and immunostained with an anti-FLAG antibody to detect the MKK6 as described in MATERIALS AND METHODS. At least 100 MKK6-transfected cells were counted in randomly selected fields for each condition and the bars represent the mean ± SEM of three independent experiments.

GFP-Bax were treated with nocodazole (3 $\mu$M) for 24 h and subsequently stained with an antibody to cytochrome *c* to detect the mitochondria (Figure 8, F–I). After 24 h of exposure to nocodazole between 20 and 30% of the transfected, mitotic cells displayed a punctate, perinuclear distribution of Bax (Figure 8F), which overlapped with a mitochondrial-rich region of the cell (Figure 8G). These cells were undergoing apoptosis as assessed by the presence of fragmented chromatin (Figure 8H). In nocodazole-arrested, nonapoptotic cells GFP-Bax was distributed homogeneously throughout the cytoplasm and did not colocalize with the mitochondria, which were distributed concentrically around the condensed chromatin (our unpublished data). Control nocodazole-arrested mitotic cells expressing GFP alone (Fig-

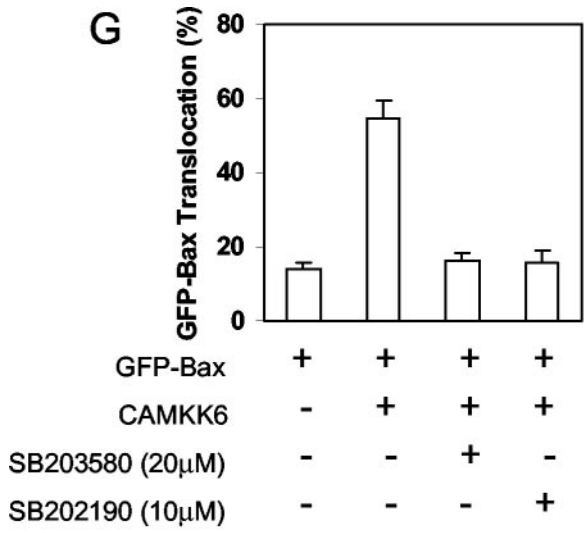


**Figure 7 (cont).**

ure 8, J–M) also did not show a punctate, perinuclear pattern of Bax fluorescence despite being clearly apoptotic, based on membrane blebbing (Figure 8J) and DNA fragmentation (Figure 8L). These experiments indicated that Bax translocates from the cytoplasm to the mitochondria in nocodazole-arrested mitotic cells as they undergo apoptosis.

Consistent with previous data regarding Bad phosphorylation by PAK (Schurmann *et al.*, 2000), our studies have indicated that recombinant PAK$\alpha$ and native PAK$\alpha$, immunoprecipitated from nocodazole-arrested mitotic cells, both efficiently phosphorylated recombinant GST-mBad (our unpublished data). Because our current data have shown that PAK$\alpha$ is activated in mitotically arrested cells, we evaluated whether Bad is also phosphorylated in this cell population. Western blots of native Bad indicated that the mobility of the Bad protein was retarded preferentially in the mitotically arrested cells, suggesting that Bad undergoes posttranslational modification in this population (Figure 9A). To assess the phosphorylation state of Bad in the mitotically arrested cells HeLa cells were transfected with a mammalian expression vector encoding GST-Bad and then treated with either nocodazole, taxol, vincristine, or vinblastine. The phosphorylation state of Bad in the mitotic and attached cell populations was assessed by immunoblotting with phospo-specific Bad antibodies, which specifically detect Bad phosphorylation on serine 112 (S112), serine 136 (S136), or serine 155 (S155). All four drug treatments induced an increase in the level of Bad phosphorylation on residues S116, S136, and S155 in the mitotically arrested cells in comparison with either the asynchronous or attached populations, although we did not detect a mobility shift with GST-Bad (Figure 9B). To determine whether one or more of the serine residues was a specific target for PAK, we coexpressed GST-mBAD with either DAPAK (L107F) or KDPAK (K298A) and then assessed the phosphorylation state of GST-mBad by immunoblotting. DAPAK did not seem to affect the phosphorylation state of Bad on either S112 or S136. However, DAPAK increased phosphorylation of Bad at S155 compared with basal Bad phosphorylation at this site or when coexpressed with KDPAK (Figure 9C). Furthermore, this phosphorylation was abolished when S155 was replaced with alanine by site-directed mutagenesis, confirming that PAK phosphorylates mBad at this site. However, basal phosphorylation of Bad (S155A) at S112 and S136 was still observed although its level was slightly reduced compared with wild-type Bad. To suppress PAK activation we used GST-PAK (amino acids 83–149 of PAK1) an inhibitor of PAK1, PAK2, and PAK3 (our unpublished data). Coexpression of GST-PAK (83–149) with GST-Bad reduced phosphorylation of Bad at S112, S136, and S155 (Figure 9D) in nocodazole-arrested mitotic cells. Expression of GST-PAK (83–149) also sensitized nocodazole-arrested mitotic cells to cell death over the time course examined compared with cells transfected with vector alone (Figure 9E). Together, these results suggest that PAK phosphorylation of Bad may be a mechanism by which PAK contributes to cell survival in mitotically arrested cells.

## DISCUSSION

We have identified the signaling events associated with activation of the spindle checkpoint by drugs that perturb microtubule dynamics. The results of this study demonstrate that 1) chemotherapeutic drugs cause activation of both p38 MAPK and PAK preferentially in the mitotically arrested cells; 2) chemotherapeutic drug-induced cell death is mediated through p38 MAPK, whereas chemotherapeutic drug-induced cell survival is mediated through PAK; 3) p38 MAPK activity induces the translocation of the cell death activator Bax, from the cytosol to the mitochondria; and 4) PAK phosphorylates Bad, thereby providing a mechanism to inhibit its proapoptotic function.

Our data indicate that the mitotic checkpoint is activated in nocodazole-arrested cells as assessed by the presence of the checkpoint protein MAD2 on the condensed chromatin. In these mitotic checkpoint-arrested cells, we demonstrate for the first time the concomitant activation of both p38 MAPK and PAK. Activation of either p38 MAPK or PAK was not observed in the attached cell population where both JNK and the Erk MAP kinases were found to be activated. The function of either JNK or Erk in the attached population is currently unknown. However, our studies indicate that Erk may suppress JNK-mediated cell death in this cell population (our unpublished data). Previous studies that have examined chemotherapeutic drug-activated signaling pathways have reported activation of JNK, p38 MAPK and Erk MAP kinases either alone or in combination (Wang *et al.*, 1998; Shtil *et al.*, 1999; Subbaramaiah *et al.*, 2000; McDaid and Horwitz, 2001; Okano and Rustgi, 2001; Seidman *et al.*, 2001; Stadheim *et al.*, 2001). Discrepancies between the signaling pathways that are activated by chemotherapeutic agents may relate to the fact that these earlier studies did not separate the mitotic and the nonmitotic cell populations. The data presented in this study suggest that there is a remarkable divergence in the signaling pathways activated by antimicrotubule drugs in these two cell populations.

The upstream signaling events that lead to the activation of p38 MAPK and PAK during mitotic arrest remain to be identified. Although it has been reported that PAKs can activate p38 MAPK (Bagrodia *et al.*, 1995), our data indicate that p38 MAPK and PAK activation are likely to be independent events. First, cotransfection of a DAPAK with p38$\alpha$

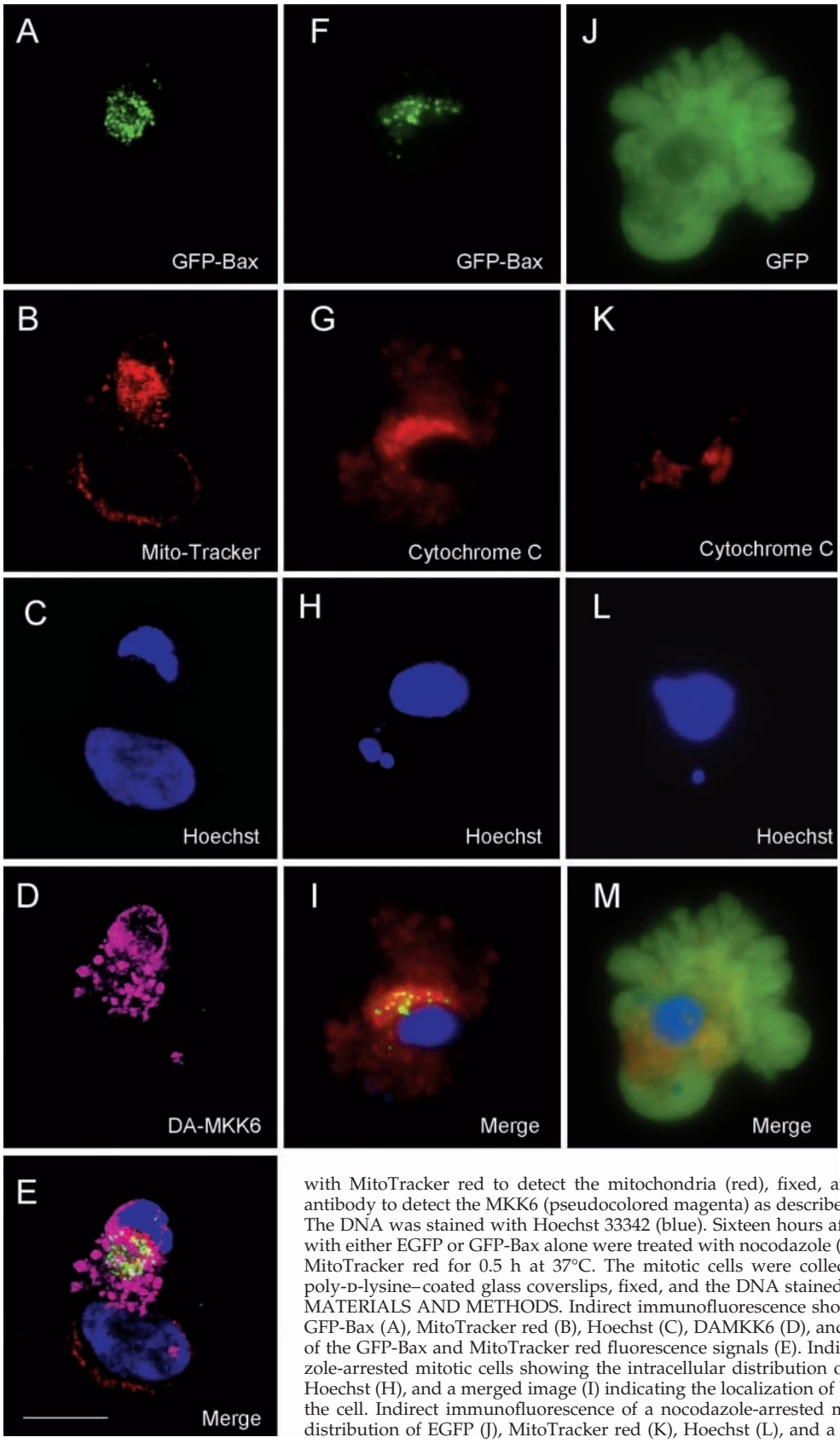


**Figure 8.** Both DAMKK6 and nocodazole induce Bax translocation to the mitochondria. Exponentially growing HeLa cells were cotransfected with GFP-Bax and FLAG-DAMKK6 (A–E) or with either GFP-Bax (F–I) or EGFP (J–M) alone. Sixteen hours after transfection, the cells cotransfected with GFP-Bax and FLAG-DAMKK6 were stained with MitoTracker red to detect the mitochondria (red), fixed, and immunostained with anti-FLAG antibody to detect the MKK6 (pseudocolored magenta) as described in MATERIALS AND METHODS. The DNA was stained with Hoechst 33342 (blue). Sixteen hours after transfection, the cells transfected with either EGFP or GFP-Bax alone were treated with nocodazole (3 $\mu$M) for 12 h and then stained with MitoTracker red for 0.5 h at 37°C. The mitotic cells were collected by shake-off and reattached to poly-D-lysine–coated glass coverslips, fixed, and the DNA stained with Hoechst 33342 as described in MATERIALS AND METHODS. Indirect immunofluorescence showing the intracellular localization of GFP-Bax (A), MitoTracker red (B), Hoechst (C), DAMKK6 (D), and a merged image indicating overlap of the GFP-Bax and MitoTracker red fluorescence signals (E). Indirect immunofluorescence of nocodazole-arrested mitotic cells showing the intracellular distribution of GFP-Bax (F), MitoTracker red (G), Hoechst (H), and a merged image (I) indicating the localization of Bax to a mitochondrial-rich region of the cell. Indirect immunofluorescence of a nocodazole-arrested mitotic cell showing the intracellular distribution of EGFP (J), MitoTracker red (K), Hoechst (L), and a merged image (M). Bar, 10 $\mu$m.

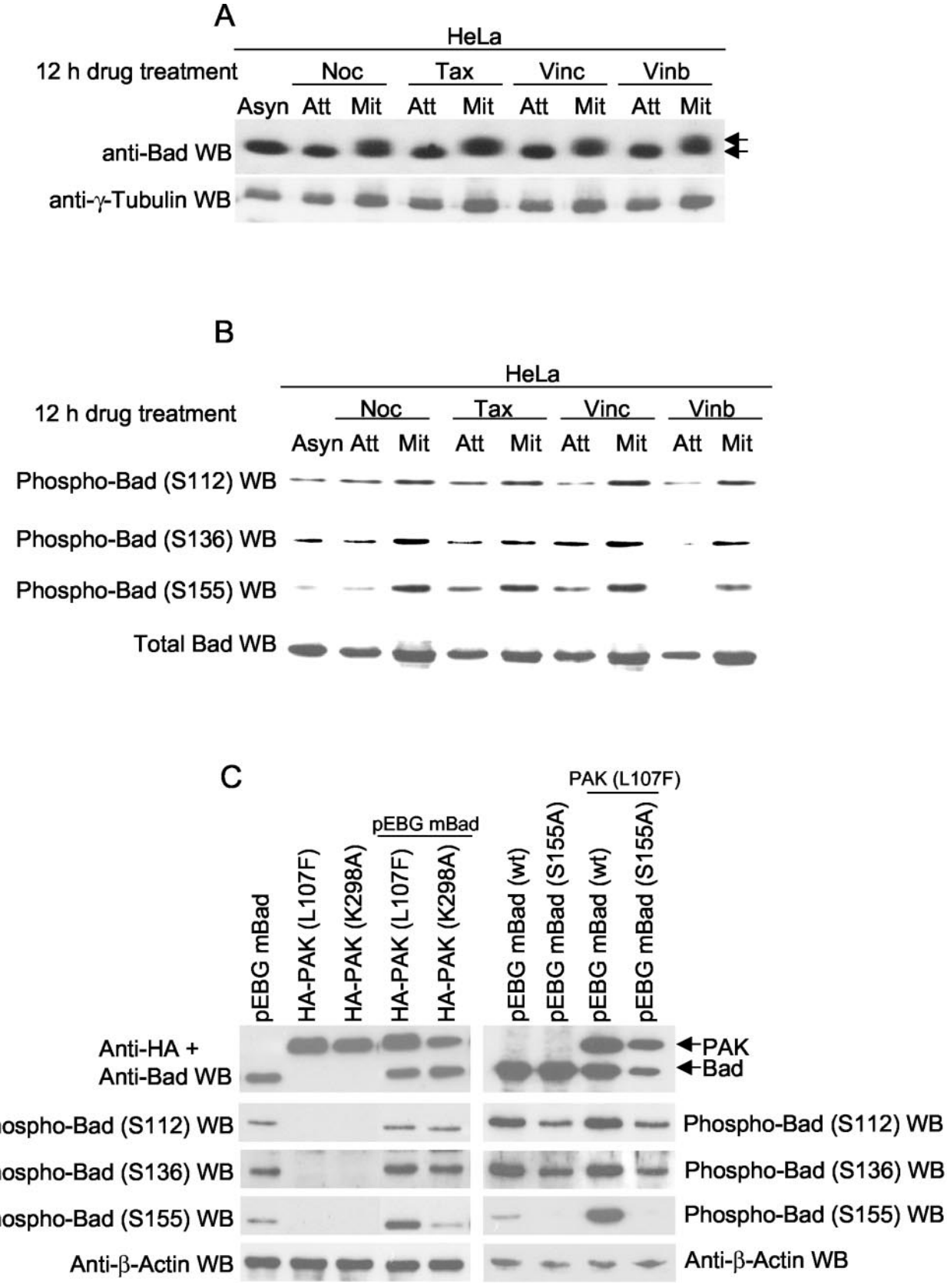
A
HeLa
12 h drug treatment
Noc
Tax
Vinc
Vinb
Asyn Att Mit Att Mit Att Mit Att Mit
anti-Bad WB
anti-γ-Tubulin WB
B
HeLa
12 h drug treatment
Noc
Tax
Vinc
Vinb
Asyn Att Mit Att Mit Att Mit Att Mit
Phospho-Bad (S112) WB
Phospho-Bad (S136) WB
Phospho-Bad (S155) WB
Total Bad WB
C
PAK (L107F)
pEBG mBad
pEBG mBad
HA-PAK (L107F)
HA-PAK (K298A)
HA-PAK (L107F)
HA-PAK (K298A)
pEBG mBad (wt)
pEBG mBad (S155A)
pEBG mBad (wt)
pEBG mBad (S155A)
Anti-HA +
Anti-Bad WB
PAK
Bad
Phospho-Bad (S112) WB
Phospho-Bad (S136) WB
Phospho-Bad (S155) WB
Anti-β-Actin WB
Phospho-Bad (S112) WB
Phospho-Bad (S136) WB
Phospho-Bad (S155) WB
Anti-β-Actin WB

**Figure 9.**

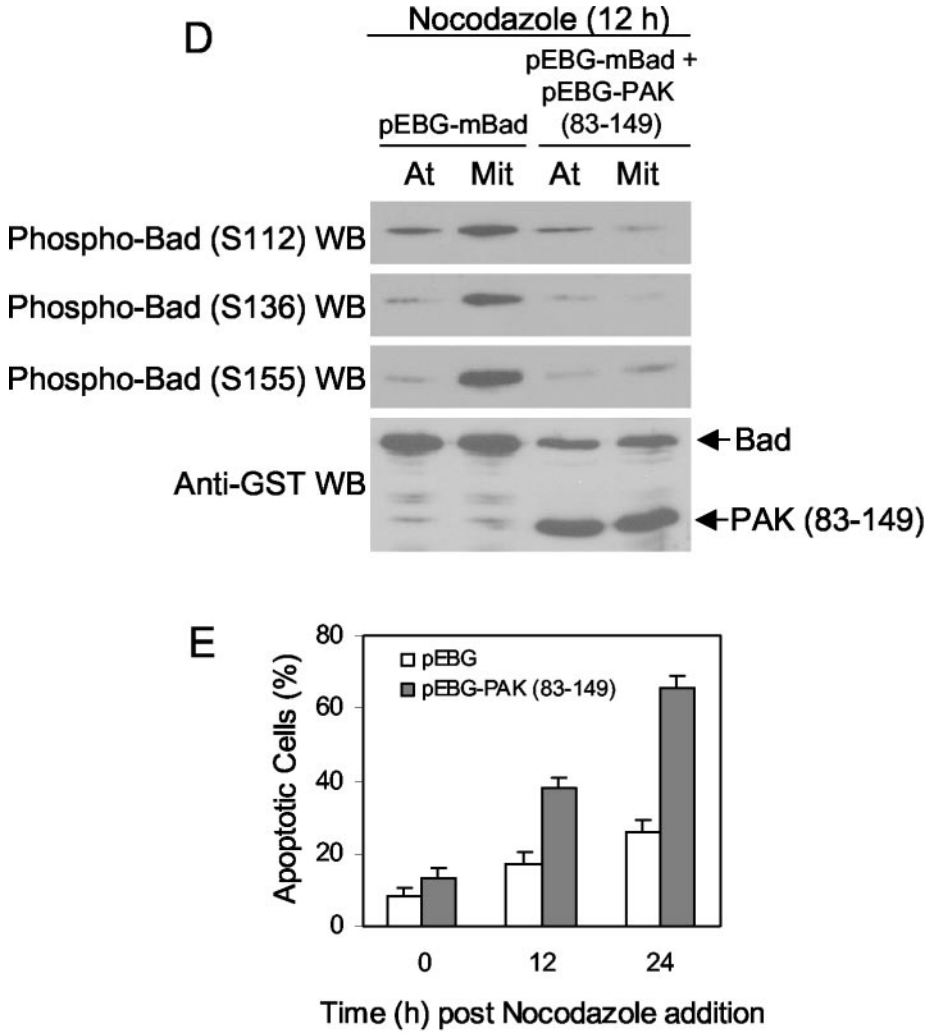


**Figure 9 (cont).** PAK phosphorylates the proapoptotic protein Bad. (A) Immunoblot analysis of native Bad after treatment of HeLa cells with nocodazole (Noc, 3 $\mu$M), taxol (Tax), vincristine (Vinc), or vinblastine (Vinb) (all 1 $\mu$M) for 12 h. The cell extracts were also immunoblotted with an anti-$\gamma$-tubulin antibody. The upper and lower arrowheads indicate the positions of the slower and faster migrating form of Bad, respectively. Asynchronous, untreated cells (Asynch), mitotic (Mit), and attached (Att). (B) Immunoblot analysis of GST-mBad phosphorylation after treatment of HeLa cells with the indicated drugs as described in (A). HeLa cells were transfected with pEBGmBAD and 24 h later treated with the indicated drugs. Cell extracts were immunoblotted with the indicated phospho-specific Bad antibodies and an anti-Bad antibody. (C) HeLa cells were transfected with pEBGmBAD wild-type, pEBGmBAD (S155A), HA-DAPAK (L107F), or HA-KDPAK (K298A) alone or in the indicated combinations. Twenty-four hours after transfection cell extracts were prepared and immunoblotted with either anti-HA, anti-Bad antibody, phospho-specific Bad antibodies, or an anti-$\beta$-actin antibody. The arrowheads indicate the positions of the Bad and PAK proteins. (D) HeLa cells were transfected with pEBGmBAD wild-type alone or in combination with pEBG-PAK (83–149). Twenty-four hours after transfection, cells were treated with nocodazole (3 $\mu$M) for 12 h. Cell extracts of the mitotic and attached populations were immunoblotted with either phospho-specific Bad antibodies or a GST antibody. The arrowheads indicate the positions of the Bad and PAK proteins. (E) HeLa cells were transfected with pEBG-PAK (83–149) or vector alone (pEBG). Twenty-four hours after transfection the cell were treated with nocodazole (3 $\mu$M) for 12 h. The mitotic cells were fixed and immunostained with an anti-GST antibody to identify the transfected cells and with the M30 antibody to identify the apoptotic cells as described in MATERIALS AND METHODS. At least 100 GST-positive cells were counted in randomly selected fields and the bars represent the mean ± SEM of three independent experiments.

did not activate the p38 MAPK. Second, p38 MAPK was inactivated before PAK, after release of cells from a mitotic block, suggesting that PAK does not regulate the activation of p38 MAPK in mitotically arrested cells. We are currently examining the upstream components of the p38 MAPK and PAK signaling pathways in mitotically arrested cells.

The downstream target(s) of p38 MAPK that cause cell death in the mitotically arrested cells are largely unknown. A recent observation (Ghatan *et al.*, 2000) that p38 MAPK induces apoptosis in neuronal cells by regulating the translocation of Bax from the cytoplasm to the mitochondria led us to examine the effect of p38 MAPK on Bax in the mitotically arrested cells. The translocation of Bax from the cytoplasm to the mitochondria is both necessary and sufficient to induce apoptotic cell death (Hsu *et al.*, 1997; Wolter *et al.*, 1997; Nechustan *et al.*, 1999). Bax reduces mitochondrial membrane potential, causes the release of cytochrome *c* from the mitochondria and activates caspases (Xiang *et al.*, 1996; Eskes *et al.*, 1998; Jurgensmeier *et al.*, 1998; Desagher *et al.*, 1999; Finucane *et al.*, 1999). In this study we demonstrate, first, that DAMKK6 causes the translocation of Bax to mitochondria, an effect that is reversed by the p38 MAPK inhibitors. Second, we show that Bax also translocates to mitochondria in the mitotically arrested cells and that the p38 MAPK inhibitors are able to suppress nocodazole-induced apoptosis. Therefore, our data support the conclusion that Bax translocation to the mitochondria, and subsequent cell death, are regulated by p38 MAPK in the mitotically blocked cells. The mechanism by which p38 MAPK may affect the cellular distribution of Bax is currently under investigation.

The activation of PAK$\alpha$ by chemotherapeutic drugs in a mitotically arrested cell population has not been described previously. We have shown in this study that DAPAK$\alpha$ suppresses MKK6-induced apoptosis, suggesting that one

function of native PAK$\alpha$ may be to suppress cell death in the mitotically blocked cells. Indeed, our data have shown that expression of DAPAK$\alpha$ confers a survival advantage during nocodazole-induced mitotic arrest, whereas inhibition of PAK activation enhances nocodazole-induced cell death. In mammalian cells PAK isoforms have been shown to play distinct roles in apoptosis. Both PAK1 (PAK$\alpha$) and PAK4 have been shown to protect cells from apoptosis induced by serum withdrawal, UV irradiation, or tumor necrosis factor-$\alpha$ in fibroblasts, or by growth factor withdrawal in lymphoid cells (Schurmann *et al.*, 2000; Tang *et al.*, 2000; Gnesutta *et al.*, 2001), whereas a *Xenopus* PAK (X-PAK1) is required to suppress apoptosis during prophase arrest in frog oocytes (Faure *et al.*, 1997). However, $\gamma$PAK (PAK2) seems to have both an antiapoptotic and a proapoptotic function (Jakobi *et al.*, 2001). The proapoptotic function of $\gamma$PAK has been attributed to the generation of constitutively active fragment after caspase-mediated cleavage of $\gamma$PAK (Rudel and Bokoch, 1997). Although the activation of both $\gamma$PAK and PAK4 in mitotically arrested cells awaits investigation the results from the present study are consistent with reports demonstrating that PAK$\alpha$ mediates cell survival in response to diverse apoptotic stimuli.

The target(s) of PAK$\alpha$ that regulate cell survival in mitotically blocked cells are also unknown. One mechanism through which PAK may protect lymphoid progenitor cells from apoptosis, after growth factor withdrawal, is by phosphorylation of the BH3-only proapoptotic protein Bad (Schurmann *et al.*, 2000). PAK is reported to phosphorylate Bad on serine residues 112 and 136, thereby facilitating binding to 14-3-3$\tau$ and its sequestration in the cytoplasm. However, other prosurvival signals are also reported to phosphorylated Bad (Downward, 1999). For example, protein kinase B phosphorylates Bad on serine residue 136, whereas protein kinase A is reported to phosphorylate Bad at serine 112. Both serine residues 112 and 136 occur within a protein kinase A phosphorylation motif (RRXS) in the BH3 domain of Bad that mediates its death-promoting activity through heterodimerization to the Bcl-XL family members (Tan *et al.*, 2000). In this study, we report that Bad is phosphorylated on serine residue 155 in addition to serine residues 112 and 136 in the mitotically arrested cells. Serine residue 155 also lies within the BH3 domain of Bad and is found in the sequence motif RRXS (Tan *et al.*, 2000) that is used by PAK to phosphorylate both serine residues 112 and 136. In overexpression experiments, we have shown that DAPAK primarily phosphorylates S155 of Bad. Phosphorylation of Bad at S155 is reported to induce cell survival by preventing the BH3-dependent dimerization of Bad with Bcl-XL rather than promoting binding to 14-3-3 (Tan *et al.*, 2000). Therefore, one mechanism by which cell death is inhibited in the mitotically arrested cells may be through phosphorylation of Bad by PAK at S155, thereby suppressing the proapoptotic Bad-Bcl-XL dimerization. We have shown that inhibition of PAK in mitotically arrested cells suppresses phosphorylation of Bad not only at S155 but also at S112 and S136 implying that native PAK is able to phosphorylate all three sites in vivo.

In summary, the present study provides evidence that both cell survival and cell death pathways are activated in mitotically arrested cells. A p38 MAPK-activated and Bax-dependent pathway contributes to cell death, whereas a PAK-activated and Bad-dependent pathway contributes to cell survival. The results of our study have implications for the design of future chemotherapeutic drug therapies that target the mitotic checkpoint. In particular, the identification of other survival pathways that are activated in response to the chemotherapeutic agents, and a search for agents that suppress them may considerably increase the effectiveness of the current anticancer therapies.

## ACKNOWLEDGMENTS

We thank Ed Manser, Roger Davis, Jiahuai Han, Gary Bokoch, and Richard Youle for generously providing various expression plasmids. Roger Snowden for assistance with flow cytometry and Kulvinder Sikand for assistance with confocal microscopy. This work was supported by grants from the Wellcome Trust and the Biotechnology and Biological Sciences Research Council (to R.P. and J.L.B.).

## REFERENCES

Aoshiba, K., Yasui, S., Hayashi, M., Tamaoki, J., and Nagai, A. (1999). Role of p38-mitogen-activated protein kinase in spontaneous apoptosis of human neutrophils. J. Immunol. *162*, 1692–1700.

Bagrodia, S., and Cerione, R.A. (1999). PAK to the future. Trends Cell Biol. *9*, 350–355.

Bagrodia, S., Derijard, B., Davis, R.J., and Cerione, R.A. (1995). Cdc42 and PAK-mediated signaling leads to Jun kinase and p38 mitogen-activated protein kinase activation. J. Biol. Chem. *270*, 27995–27998.

Bueno, O.F., *et al.* (2000). The MEK1-ERK1/2 signaling pathway promotes compensated cardiac hypertrophy in transgenic mice. Cancer Res. *60*, 5887–5894.

Burke, D. (2000). Complexity in the spindle checkpoint. Curr. Opin. Gen. Dev. *10*, 26–31.

Communal, C., Colucci, W.S., and Singh, K. (2000). p38 Mitogen-activated protein kinase pathway protects adult rat ventricular myocytes against $\beta$-adrenergic receptor-stimulated apoptosis. Evidence for $G_i$-dependent activation. J. Biol. Chem. *275*, 19395–19400.

Derijard, B., Raingeaud, J., Barrett, T., Wu, I.H., Han, J., Ulevitch, R.J., and Davis, R.J. (1995). Independent human MAP-kinase signal transduction pathways defined by MEK and MKK isoforms. Science *270*, 7420–7426.

Desagher, S., Osen-Sand, A., Nichols, A., Eskes, R., Montessuit, S., Lauper, S., Maundrell, K., Antonsson, B., and Martinou, J.C. (1999). Bid-induced conformational change of Bax is responsible for mitochondrail cytochrome c release during apoptosis. J. Cell Biol. *144*, 891–901.

Deacon, K., and Blank, J.L. (1999). MEK kinase 3 directly activates MKK6 and MKK7, specific activators of the p38 and c-Jun $NH_2$-terminal kinases. J. Biol. Chem. *274*, 16604–16610.

Deschesnes, R.G., Huot, J., Valerie, K., and Landry, J. (2001). Involvement of p38 in apoptosis-associated membrane blebbing and nuclear condensation. Mol. Biol. Cell *12*, 1569–1582.

Downward, J. (1999). How BAD phosphorylation is good for survival. Nat. Cell Biol. *1*, E33–E35.

Eskes, R., Antonsson, B., Osen-Sand, A., Montessuit, S., Richter, C., Sadoul, R., Mazzei, G., Nichols, A., and Martinou, J.C. (1998). Bax-induced cytochrome c release from mitochondria is independent of the permeability transition pore but highly dependent on $Mg^{2+}$ ions. J. Cell Biol. *143*, 217–224.

Fang, G., Yu, H., and Kirschner, M.W. (1999). Control of mitotic transitions by the anaphase-promoting complex. Phil. Trans. R. Soc. Lond. B. Biol. Sci. *354*, 1583–1590.

Faure, S., Vigneron, S., Doree, M., and Morin, N. (1997). A member of the Ste20/PAK family of protein kinases is involved in both arrest in *Xenopus* oocytes and G2/prophase of the first meiotic cell cycle and prevention of apoptosis. *EMBO J. 16*, 5550–5561.

Finucane, D.M., Bossy-Wetzel, E., Waterhouse, N.J., Cotter, T.G., and Green, D.R. (1999). Bax-induced caspase activation and apoptosis via cytochrome c release from mitochondria is inhibitable by Bcl-xL. J. Biol. Chem. *274*, 2225–2233.

Geley, S., Kramer, E., Gieffers, C., Gannon, J., Peters, J.M., and Hunt, T. (2001). Anaphase-promoting complex/cyclosome-dependent proteolysis of human cyclin A starts at the beginning of mitosis and is not subject to the spindle assembly checkpoint. J. Cell Biol. *153*, 137–148.

Ghatan, S., Larner, S., Kinoshita, Y., Hetman, M., Patel, L., Xia, Z., Youle, R.J., and Morrison, R.S. (2000). p38 MAPK mediates Bax translocation in nitric oxide-induced apoptosis in neurons. J. Cell Biol. *150*, 335–347.

Gnesutta, N., Qu, J., and Minden, A. (2001). The serine/threonine kinase PAK4 prevents caspase activation and protects cells from apoptosis. J. Biol. Chem. *276*, 14414–14419.

Hagemann, C., and Blank, J.L. (2001). The ups and downs of MEK kinase interactions. Cell Signal. *13*, 863–875.

Hsu, Y.T., Wolter, K.G., and Youle, R.J. (1997). Cytosol-to-membrane redistribution of Bax and Bcl-X(L) during apoptosis. Proc. Natl. Acad. Sci. USA *94*, 3668–3672.

Jakobi, R., Moertl, E., and Koeppel, M.A. (2001). p21-activated protein kinase γ-PAK suppresses programmed cell death of BALB3T3 fibroblasts. J. Biol. Chem. *276*, 16624–16634.

Jiang, Y., Gram, H., Zhao, M., New, L., Gu, J., Feng, L., DiPadova, F., Ulevitch, R.J., and Han, J. (1997). Characterization of the structure and function of the fourth member of p38 group mitogen-activated protein kinases, p38δ. J. Biol. Chem. *272*, 30122–30128.

Jordan, M.A., Wendell, K., Gardiner, S., Derry, W.B., Copp, H., and Wilson, L. (1996). Mitotic block induced in HeLa cells by low concentrations of paclitaxel (Taxol) results in abnormal mitotic exit and apoptotic cell death. Cancer Res. *56*, 816–825.

Jurgensmeier, J.M., Xie, Z., Devereaux, Q., Ellerby, L., Bredesen, D., and Reed, J.C. (1998). Bax directly induces release of cytochrome c from isolated mitochondria. Proc. Natl. Acad. Sci. USA *95*, 4997–5002.

Kyriakis, J.M., and Avruch, J. (2001). Mammalian mitogen-activated protein kinase signal transduction pathways activated by stress and inflammation. Physiol. Rev. *81*, 807–869.

Kummer, J.L., Rao, P.K., and Heidenreich, K.A. (1997). Apoptosis induced by withdrawal of trophic factors is mediated by p38 mitogen-activated protein kinase. J. Biol. Chem. *272*, 20490–20494.

Kurokawa, H., Lenferink, A.E., Simpson, J.F., Pisacane, P.I., Sliwkowski, M.X., Forbes, J.T., and Arteaga, C.L. (2000). Inhibition of HER2/Neu (erbB-2) and mitogen-activated protein kinases enhance tamoxifen action against HER2-overexpressing, tamoxifen-resistant breast cancer cells. Cancer Res. *60*, 5887–5894.

Leers, M.P.G., *et al*. (1999). Immunocytochemical detection and mapping of a cytokeratin 18 neo-epitope exposed during early apoptosis. J. Pathol. *187*, 567–572.

Lee, J.C., *et al*. (1994). A protein kinase involved in the regulation of inflammatory cytokine biosynthesis. Nature *372*, 739–746.

Li, Y., and Benezra, R. (1996). Identification of a human mitotic checkpoint gene: hsMAD2. Science *274*, 246–248.

McDaid, H.M., and Horwitz, S.B. (2001). Selective potentiation of paclitaxel (taxol)-induced cell death by mitogen-activated protein kinase kinase inhibition in human cell lines. Mol. Pharmacol. *60*, 290–301.

Nechustan, A., Smith, C.L., Hsu, Y.T., and Youle, R.J. (1999). Conformation of the Bax C-terminus regulates subcellular location and cell death. EMBO J. *273*, 16415–16420.

Okano, J.-I., and Rustgi, A.K. (2001). Paclitaxel induces prolonged activation of the Ras/MEK/ERK pathway independently of activating the programmed cell death machinery. J. Biol. Chem. *276*, 19555–19564.

Patel, R., Bartosch, B., and Blank, J.L. (1998). $p21^{WAF1}$ is dynamically associated with JNK in human T-lymphocytes during cell cycle progression. J. Cell Sci. *111*, 2247–2255.

Patel, R., Holt, M., Philipova, R., Moss, S., Schulman, H., Hidaka, H., and Whitaker, M. (1999). Calcium/calmodulin-dependent phosphorylation and activation of human cdc25-C at the G2/M phase transition in HeLa cells. J. Biol. Chem. *274*, 7958–7968.

Potapova, O., Haghighi, A., Bost, F., Liu, C., Birrer, M.J., Gjerset, R., and Mercola, D. (1997). The Jun kinase/stress-activated protein kinase pathway functions to regulate DNA repair and inhibition of the pathway sensitizes tumor cells to cisplatin. J. Biol. Chem. *272*, 14041–14044.

Remacle-Bonnet, M.M., Garrouste, F.L., Heller, S., Andre, F., Marvaldi, J.L., and Pommier, G.J. (2000). Insulin-like growth factor-1 protects colon cancer cells from death factor-induced apoptosis by potentiating tumor necrosis factor α-induced mitogen-activated protein kinase and nuclear factor κB signaling pathways. Cancer Res. *60*, 2007–2017.

Rowinsky, E.K., and Donehower, R.C. (1991). The clinical pharmacology and use of antimicrotubule agents in cancer chemotherapy. Pharmacol. Ther. *52*, 35–84.

Rudel, T., and Bokoch, G.M. (1997). Membrane and morphological changes in apoptotic cells regulated by caspase-mediated activation of PAK2. Science *276*, 1571–1574.

Schurmann, A., Mooney, A.F., Sanders, L.C., Sells, M.A., Wang, H.G., Reed, J.C., and Bokoch, G.M. (2000). P21-activated kinase 1 phosphorylares the death agonist Bad and protects cells from apoptosis. Mol. Cell. Biol. *20*, 453–461.

Seidman, R., Gitelman, I., Sagi, O., Horwitz, S.B., and Wolfson, M. (2001). The role of erk1/2 and p38 MAP-kinase pathways in taxol-induced apoptosis in human ovarian carcinoma cells. Exp. Cell Res. *268*, 84–92.

Shah, J.V., and Cleveland, D.W. (2000). Waiting for anaphase: Mad2 and the spindle assembly checkpoint. Cell *103*, 997–1000.

Shtil, A.A., Mandlekar, S., Yu, R., Walter, R.J., Hagen, K., Tan, T.H., Roninson, I.B., and Kong, A.N. (1999). Differential regulation of mitogen-activated protein kinases by microtubule-binding agents in human breast cancer cells. Oncogene *18*, 377–384.

Sorger, P.K., Dobles, M., Tournebize, R., and Hyman, A.A. (1997). Coupling cell division and cell death to microtubule dynamics. Curr. Opin. Cell Biol. *9*, 807–814.

Stadheim, T.A., Xiao, H., and Eastman, A. (2001). Inhibition of extracellular signal-regulated kinase (ERK) mediates cell cycle phase independent apoptosis in vinblastine-treated ML-1 cells. Cancer Res. *61*, 1533–1540.

Subbaramaiah, K., Hart, J.C., Norton, L., and Dannenberg, A.J. (2000). Microtubule-interfering agents stimulate the transcription of cyclo-oxygenase-2. Evidence for involvement of ERK1/2 and p38 mitogen-activated protein kinase pathways. J. Biol. Chem. *275*, 14838–14845.

Tang, Y., Zhou, S., Chen, A., Pittman, R.N., and Field, J. (2000). The Akt proto-oncogene links Ras to Pak and cell survival signals. J. Biol. Chem. *275*, 9106–9109.

Tan, Y., Demeter, M.R., Ruan, H., and Comb, M.J. (2000). BAD Ser-155 phosphorylation regulates BAD/Bcl-XL interaction and cell survival. J. Biol. Chem. *275*, 25865–25869.

Verheij, M., *et al*. (1996). Requirement for ceramide-initiated SAPK/JNK signaling in stress-induced apoptosis. Nature *380*, 75–79.

Wang, T.H., Wang, H.S., Ichijo, H., Giannakakou, P., Foster, J.S., Fojo, T., and Wimalasena, J. (1998). Microtubule-interfering agents activate c-Jun N-terminal kinase/stress-activated protein kinase through both ras and apoptosis signal-regulating kinase pathways. J. Biol. Chem. *273*, 4928–4936.

Wang, T.H., Wang, H.S., and Soong, Y.K. (2000). Paclitaxel-induced cell death: where the cell cycle and apoptosis come together. Cancer *88*, 2619–2628.

Wilson, L., and Jordan, M.A. (1995). Microtubule dynamics: taking aim at a moving target. Chem. Biol. *2*, 569–573.

Wolter, K.G., Hsu, Y-T., Smith, C.L., Nechustan, A., Xi, X.G., and Youle, R.J. (1997). Movement of bax from the cytosol to mitochondria during apoptosis. J. Cell Biol. *139,* 1281–1292.

Woods, C.M., Zhu, J., McQuenet, P.A., Bollag, D., and Lazarides, E. (1995). Taxol-induced mitotic block triggers rapid onset of a p53-independent apoptotic pathway. Mol. Med. *1,* 506–526.

Xia, Z., Dickens, M., Raingeaud, J., Davis, R.J., and Greenberg, M.E. (1995). Opposing effects of ERK and JNK-p38 MAPKs on apoptosis. Science *270*, 1326–1331.

Xiang, J.G., Chao, D.T., and Korsmeyer, S.J. (1996). BAX-induced cell death may not require interleukin IL$\beta$-converting enzyme-like proteases. Proc. Natl. Acad. Sci. USA *93*, 14559–14563.

Yujiri, T., Fanger, G.R., Garrington, T.P., Schlesinger, T.K., Gibson, S., and Johnson, G.L. (1999). MEK kinase 1 (MEKK1) transduces c-Jun $NH_2$-terminal kinase activation in response to changes in the microtubule cytoskeleton. J. Biol. Chem. *272*, 12605–12610.